Linda Yip,[1] Rebecca Fuhlbrigge,[1] Cariel Taylor,[1] Remi J. Creusot,[2] Teppei Nishikawa-Matsumura,[1] Chan C. Whiting,[1] Jill M. Schartner,[1] Rahima Akter,[1] Matthias von Herrath,[3] and C. Garrison Fathman[1]

Inflammation and Hyperglycemia Mediate *Deaf1* Splicing in the Pancreatic Lymph Nodes via Distinct Pathways During Type 1 Diabetes

Diabetes 2015;64:604–617 | DOI: 10.2337/db14-0803

PATHOPHYSIOLOGY

Peripheral tolerance is partially controlled by the expression of peripheral tissue antigens (PTAs) in lymph node stromal cells (LNSCs). We previously identified a transcriptional regulator, deformed epidermal autoregulatory factor 1 (Deaf1), that can regulate PTA expression in LNSCs of the pancreatic lymph nodes (PLNs). During the pathogenesis of type 1 diabetes (T1D), *Deaf1* is spliced to form the dominant-negative isoform *Deaf1-Var1*. Here we show that *Deaf1-Var1* expression correlates with the severity of disease in NOD mice and is reduced in the PLNs of mice that do not develop hyperglycemia. Inflammation and hyperglycemia independently drive *Deaf1* splicing through activation of the splicing factors *Srsf10* and *Ptbp2*, respectively. Inflammation induced by injection of activated splenocytes increased *Deaf1-Var1* and *Srsf10,* but not *Ptbp2*, in the PLNs of NOD.SCID mice. Hyperglycemia induced by treatment with the insulin receptor agonist S961 increased *Deaf1-Var1* and *Ptbp2*, but not *Srsf10*, in the PLNs of NOD.B10 and NOD mice. Overexpression of *PTBP2* and/or *SRSF10* also increased human *DEAF1-VAR1* and reduced PTA expression in HEK293T cells. These data suggest that during the progression of T1D, inflammation and hyperglycemia mediate the splicing of *DEAF1* and loss of PTA expression in LNSCs by regulating the expression of *SRSF10* and *PTBP2.*

Type 1 diabetes (T1D) results from a combination of genetic, epigenetic, and environmental factors. During disease progression, a breakdown in self-tolerance occurs, allowing autoreactive T cells that recognize pancreatic antigens to escape deletion or inactivation and mediate the autoimmune destruction of pancreatic β-cells. Normally, deletion of naive autoreactive T cells is mediated in the thymus by medullary thymic epithelial cells that express an array of peripheral tissue antigens (PTAs) under the control of the autoimmune regulator gene (*Aire*). However, some self-reactive T cells, including those that recognize islet antigens, can escape to the periphery (1–5). These cells are dealt with by additional peripheral mechanisms. Lymph node stromal cells (LNSCs) have recently been shown to induce T-cell tolerance by ectopically expressing and presenting self-antigens in a manner comparable to medullary thymic epithelial cells (6–12). LNSCs also have been suggested to mediate the conversion of autoreactive CD4+ T cells to T regulatory cells (Tregs) (13).

The ectopic expression of genes encoding PTAs is not controlled by Aire in LNSCs (14) but instead is regulated in part by the transcriptional regulator deformed autoregulatory factor 1 (Deaf1). Deaf1 is highly enriched in LNSCs and has structural homology to Aire: it contains a DNA-binding SAND (Sp100, Aire-1, NucP41/75, and

[1]Department of Medicine, Division of Immunology and Rheumatology, Stanford University, Stanford, CA
[2]Department of Medicine, Columbia Center for Translational Immunology and Naomi Berrie Diabetes Center, Columbia University Medical Center, New York, NY
[3]Type 1 Diabetes Center, The La Jolla Institute for Allergy and Immunology, La Jolla, CA
Corresponding author: Linda Yip, lindayip@stanford.edu.

Received 20 May 2014 and accepted 26 August 2014.
This article contains Supplementary Data online at http://diabetes.diabetesjournals.org/lookup/suppl/doi:10.2337/db14-0803/-/DC1.

Deaf1) domain, which mediates chromatin-dependent transcription and protein–protein interactions (15,16), and a ZF-MYND (zinc finger, myeloid, Nervy, and Deaf1) domain that is similar to the plant homeodomain 1 of Aire. We previously showed that Deaf1 controls the transcription of hundreds of genes in the pancreatic lymph nodes (PLNs) and regulates the processing and presentation of PTA genes in LNSCs by controlling the transcription of the eukaryotic translation initiation factor 4 gamma 3 gene (*Eif4g3*) that encodes eIF4GII (17).

During the progression of T1D, Deaf1 function is diminished in the PLNs and may contribute to the pathogenesis of disease. We previously showed that *DEAF1* was alternatively spliced to form a dominant-negative isoform (*DEAF1-VAR1*) in the PLNs of human patients with T1D and of nonobese diabetic (NOD) mice (18,19). The human *DEAF1-VAR1* and mouse *Deaf1-Var1* isoforms are functionally similar: both lack the nuclear localization signal and are expressed in the cytoplasm, where they heterodimerize with and inhibit the function of the canonical isoform of Deaf1. This leads to reduced Deaf1 function and likely accounts for the diminished levels of pancreatic PTA expression observed during the progression of disease in the PLNs of NOD mice and patients with T1D. Loss of PTA expression could contribute to a breakdown in peripheral tolerance by allowing the escape and persistence of islet-reactive T cells or diminished induction of Tregs.

What induces the alternative splicing of *Deaf1* and *DEAF1* during the progression of disease in NOD mice and human T1D, respectively, is unclear. Here, we questioned whether inflammation and hyperglycemia, the hallmark traits of T1D, might be involved. We showed that both inflammation and hyperglycemia could independently mediate *Deaf1* splicing through the activation of pathways that involve the splicing factors serine/arginine-rich splicing factor 10 (Srsf10) and polypyrimidine tract binding protein 2 (Ptbp2), respectively. These findings provide valuable insight into the pathology of T1D and identify pathways that may be targeted during therapy.

RESEARCH DESIGN AND METHODS

Mice

Female NOD/LtJ (NOD), NOD.B10Sn-*H2*^{b}/J (NOD.B10), NOD.CB17-Prkdc^{scid}/J (NOD.SCID), and NOD.Cg-Tg (TcraBDC2.5)1DoiTg(TcrbBDC2.5)Doi/DoiJ (NOD.BDC2.5) mice were purchased from The Jackson Laboratory. *Deaf1* knockout and wild-type littermate BALB/c control mice were bred at the Stanford School of Medicine's animal facility (17,20). Animals were maintained under pathogen-free conditions at the facility and The La Jolla Institute for Allergy and Immunology, according to institutional guidelines for animal use and care. Female NOD mice develop autoimmune diabetes in a spontaneous and highly penetrant manner and serve as a model of human T1D. They express a number of autoantibodies in common with human patients with T1D. They also express several susceptibility genes, including the MHC class II allele I-A^{g7}, which is structurally similar to DQ8, a major T1D-associated MHC allele in humans. The MHC congenic NOD.B10 mice that express the non-disease-associated I-A^{b} allele and do not develop insulitis or diabetes served as controls. NOD.SCID mice lacking a functioning immune system were used to study the effect of inflammation on *Deaf1* splicing in the PLNs. These mice served as recipients of activated splenocytes from NOD.BDC2.5 mice; these splenocytes migrate to the PLNs. The NOD.BDC2.5 mice express the BDC2.5 T-cell receptor transgene that targets chromogranin A, a β-cell antigen, and produce CD4^{+} T cells that are highly diabetogenic when adoptively transferred into NOD.SCID mice.

Cells

HEK293T cells were purchased from the American Type Culture Collection. Lymph node stromal element (LNSE)–enriched cells and various LNSC subsets were prepared as previously described (17,19).

Dendritic Cell/Interleukin-4 Treatment of NOD Mice

NOD mice were treated with PBS, dendritic cells (DCs), or DCs that were electroporated with interleukin (IL)-4 mRNA (Argos Therapeutics), as previously described (21). *Deaf1-Var1* expression was assessed in the PLNs of 12-week-old mice 3 days after treatment with DCs transduced with interleukin (IL)-4 (DC/IL-4), DCs, and PBS (n = 10 per group), as described in RNA EXTRACTION, cDNA SYNTHESIS, AND QPCR. Blood glucose was measured in another cohort of 12-week-old mice treated with DC/IL-4 and PBS (n = 10 per group). The incidence of hyperglycemia was compared using a log-rank test (Prism 5; GraphPad Software Inc.).

Histology

Fresh frozen sections (10 μm) of the pancreas of NOD mice were cut, air-dried, and stained using HistoGene staining solution (Arcturus). Four sections obtained at 30-μm intervals were assessed per animal. Islets were counted and categorized based on the degree of insulitis.

Insulin Treatment of Hyperglycemic NOD Mice

Blood glucose of NOD mice was monitored 3 times a week starting at 8 weeks of age (n = 28). Mice with blood glucose >375 mg/dL were implanted with subcutaneous insulin pellets (LinShin Canada Inc.). Additional pellets were inserted as required to maintain survival until 24 weeks of age (Supplementary Fig. 1).

Splenocyte Activation and Adoptive Transfer of Activated Splenocytes

Splenocytes from 12-week-old female NOD.BDC2.5 or NOD.B10 mice were activated in anti-CD3/anti-CD28-coated plates (2 μg/mL) in the presence of lipopolysaccharide (1 μg/mL) and interferon (IFN)-α (200 U/mL) for 24 h, as previously described (20). Cell supernatants were analyzed by Luminex arrays (Human Immune Monitoring Center, Stanford, CT). Splenocytes (5×10^{6}) were injected intraperitoneally into 12-week-old female NOD.SCID or NOD.B10 mice. Control mice were injected with an

equal volume of PBS (200 μL). Tissues were harvested 24 h later.

S961 Treatment

Ten-week-old NOD and NOD.B10 mice were treated with the insulin receptor antagonist S961 (50 nmol/kg/h for 60 h) using intraperitoneal osmotic pumps (Alzet). The S961 was kindly provided by Dr. Lauge Schäffer (Novo Nordisk). This dosage was based on previous studies and data showing that intraperitoneal injection of 100 nmol/kg maintains hyperglycemia for ~2 h after a glucose challenge in overnight-fasted mice (22) (Supplementary Fig. 3*A*). Mice were pretreated with S961 (100 nmol/kg intraperitoneally) for 10 min before intraperitoneal glucose injection (2 g/kg).

RNA Extraction, cDNA Synthesis, and QPCR

Total RNA was extracted using Trizol reagent and the Qiagen RNeasy mini or micro kit, as previously described (17,19). Total RNA was assessed using the Agilent 2100 Bioanalyzer and the RNA 6000 Pico or Nano Reagent Kit (Agilent). First-strand cDNA was generated using Superscript III (Invitrogen). Quantitative PCR (QPCR) was performed to measure levels of expression of mouse *Deaf1*, *Srsf10*, *Ptbp2*, *Ifng*, *Cela1*, *Gapdh*, and *Actb*; human *DEAF1*, *SRSF10*, *PTBP2*; and mammalian *18S rRNA* using TaqMan gene expression assays (Applied Biosystems). Custom-designed primers (Table 1) were used to measure *Deaf1-Var1*, *DEAF1-VAR1*, and *CELA1* (19). cDNA was preamplified using the TaqMan PreAmp Mastermix (Applied Biosystems) before QPCR for measurements that gave threshold cycle (Ct) values of >30. The 7900HT Fast Real Time PCR System (Applied Biosystems) and the TaqMan Gene Expression Mastermix (Applied Biosystems) or the Veriquest Fast SYBR Green PCR Master Mix (Affymetrix) were used according to manufacturer's instructions. The comparative Ct method for relative quantification (ΔΔCt) was used.

Microarray Analysis

Microarrays were performed at the Stanford Human Immune Monitoring Center using the Whole Mouse Genome Microarray Kit, 4 × 44 K 2-color arrays (Agilent Technologies), as previously described (17,19). Gene expression was measured in the PLNs of the two 16-week-old NOD mice with the highest *Deaf1-Var1* expression (top 15th percentile) against a pooled sample of PLNs from the two mice with the lowest *Deaf1-Var1* expression (lowest 15th percentile). Data were processed with Feature Extraction software (Agilent Technologies) and analyzed using GeneSpring GX 11.5 software (Agilent Technologies). Samples were filtered for detected entities and for entities that were upregulated or downregulated in both samples. Gene ontology analysis was performed. All microarray data have been submitted to the Gene Expression Omnibus (GEO) Database at National Center for Biotechnology Information (GEO series accession no. GSE57237).

Cell Transfection

HEK293T cells were transfected with various plasmids (*SRSF10* or *PTBP2* in the pCMV6-XL5 vector or the empty pCMV6-XL5 vector; Origene) alone (1 μg) or in combination (0.5 μg each) using Lipofectamine LTX (Invitrogen), according to manufacturers' instructions. Transfected cells were lysed in Trizol reagent, and total RNA was extracted as described above. For immunoblotting, cells were lysed in M-PER mammalian protein extraction reagent containing 1× HALT protease inhibitor cocktail (Thermo Scientific).

SDS-PAGE and Immunoblotting

Protein samples were prepared in Laemmli sample buffer containing β-mercaptoethanol (Bio-Rad). SDS-PAGE and immunoblotting were performed according to standard procedures using the rabbit polyclonal anti-PTBP2 (ABE431; Millipore) at 1:2,000 and polyclonal anti-FUSIP1/SRSF10 (E-23; sc-101961; Santa Cruz Biotechnology) at 1:1,000. These antibodies may recognize multiple isoforms of PTBP2 and SRSF10. Six alternatively spliced isoforms of human SRSF10 (ranging from ~20–31 kDa) and PTBP2 (ranging from ~38 to 58 kDa) have previously been described (www.uniprot.org). β-Actin concentrations were measured as a loading control using a horseradish peroxidase–conjugated rabbit monoclonal antibody to β-actin (#13E5; Cell Signaling) at 1:1,000 and an antirabbit horseradish peroxidase secondary antibody (Zymed) at 1:15,000 diluted in StartingBlock T20 (Thermo Scientific).

Islet Isolation

Pancreatic islets were isolated from 12-week-old NOD.B10 mice, as previously described (23). To examine the effect of inflammation on *Deaf1* splicing, islets from 3–5 mice were

Table 1—Primers for QPCR

Target	GenBank Accession No.	Sequence (5′ to 3′)	Amplicon (Base Pairs)
Mouse *Deaf1-Var1* (TaqMan assay)	FJ377318	Forward: CCTTCCCTTGGCCCACTT Reverse: AAGCACACAGCCTCGACATCT Probe: FAM-TTCTACGAATCTAAAGCTC-MGB	62
Human *DEAF1-VAR1* (SYBR green assay)	FJ985253	Forward: TCGGCTCAGGATGGGATCTT Reverse: GTCACGGTGATAAGGTCATG	85
Human *CELA1* (SYBR green assay)	NM_001971	Forward: GGCTGGAGACCATAACCTGA Reverse: AACACCCAGCTGGACATAGC	172

pooled and approximately 50 individual islets were incubated for 24 h in the supernatant of activated or nonactivated 12-week-old NOD.B10 splenocytes.

Statistical Analysis

Statistical analyses were performed using the two-tailed unpaired Student *t* test (Prism 5 software). A *P* value ≤ 0.05 was considered significant.

RESULTS

Deaf1 Splicing Only Occurs in the PLNs of NOD Mice That Develop Hyperglycemia

Deaf1 splicing is increased in the PLNs of NOD versus NOD.B10 mice at the onset and during the progression of disease (19). However, it was unclear when *Deaf1* splicing occurs and whether it occurs in the PLNs of NOD mice that do not develop hyperglycemia. Approximately 20% of the female NOD mice in our colony did not develop hyperglycemia by 30 weeks of age. By 20 weeks of age, NOD mice that are still euglycemic (glucose <200 mg/dL) are likely to remain so. Here we show that *Deaf1-Var1* expression did not differ between a cohort of euglycemic 20-week-old NOD mice and age-matched euglycemic NOD.B10 mice (Fig. 1*A* and *B*).

To test whether *Deaf1* splicing occurred in mice that did not develop hyperglycemia, blood glucose was monitored in a group of 28 NOD mice until 24 weeks of age (Fig. 1*C* and *D*). Blood glucose was measured three times per week, and insulin pellets were inserted in mice with blood glucose >375 mg/dL. By 24 weeks of age, approximately 60% had developed or were trending toward sustained hyperglycemia; 8 mice that became hyperglycemic were treated with insulin pellets, 6 other mice were treated with insulin pellets but died before 24 weeks, and 3 untreated mice had blood glucose concentrations >200 mg/dL at 24 weeks (Fig. 1*D*). Eleven mice in this cohort maintained blood glucose concentrations <200 mg/dL and were not treated with insulin pellets (Fig. 1*C*). Handling and bleeding of the mice three times a week may account for the slightly lower incidence of hyperglycemia than normally seen in our colony (24). *Deaf1-Var1* expression was significantly higher in the PLNs of the 24-week-old insulin-treated NOD mice compared with age-matched NOD mice that did not develop hyperglycemia (Fig. 1*E*), demonstrating that *Deaf1* splicing is upregulated in mice that became diabetic compared with those that maintained euglycemia. The blood glucose concentrations of the hyperglycemic NOD mice decreased quickly upon insulin pellet treatment and gradually increased to >375 mg/dL, at which time another insulin pellet was administered (Supplementary Fig. 1*A*). At the time of death (24 weeks of age), the blood glucose concentrations of the diseased mice ranged from 59 to 402 mg/dL. *Deaf1-Var1* expression in the PLNs of these mice did not correlate with blood glucose concentrations at the time of death (Supplementary Fig. 1*B*). This suggested that once female NOD mice become hyperglycemic, splicing of *Deaf1* has occurred and, despite treatment with insulin pellets to modulate the hyperglycemic state and keep the mice alive, *Deaf1* remained spliced in the PLNs of these treated mice compared with the mice that did not become hyperglycemic in this experiment.

Next we examined whether *Deaf1* was spliced in the PLNs of mice that were treated to prevent the development of hyperglycemia. DC/IL-4 have previously been shown by our laboratory to prevent or delay disease in NOD mice (21) and to cause gene expression in the PLNs of DC/IL-4-treated NOD mice to become more similar to the gene expression observed in control NOD.B10 mice (25). Here we demonstrated that DC/IL-4 treatment reduced the incidence of hyperglycemia compared with that among control mice that were treated with PBS (Fig. 1*F*). Previous studies have shown that disease developed similarly in controls that were treated with PBS or with DCs that were not transfected to express IL-4 (21). We showed that DC/IL-4 treatment significantly reduced the level of *Deaf1-Var1* expression in the PLNs compared with controls treated with PBS or with only DCs (Fig. 1*G*).

Deaf1 Splicing in NOD PLNs Directly Correlates With the Severity of Disease

We then assessed *Deaf1-Var1* expression in a group of 16-week-old female NOD mice at various stages of disease and showed that *Deaf1-Var1* expression was tightly correlated with both blood glucose concentrations and the degree of insulitis (Fig. 2 and Supplementary Fig. 2). This suggested that both hyperglycemia and/or inflammation may play roles in *Deaf1* splicing. We developed the following experiments to assess how one or both of these phenomena influence *Deaf1* splicing.

Inflammation Induces the Splicing of *Deaf1* in the PLNs

We previously showed that *Deaf1-Var1* expression within the lymph nodes is approximately 10-fold higher in the LNSEs than in T or B lymphocytes (17). Thus, we compared *Deaf1-Var1* expression in the inflamed and noninflamed LNSE extracted from the PLNs of 12-week-old NOD and NOD.SCID mice, respectively. *Deaf1-Var1* expression was detected in the inflamed LNSE of NOD mice but not in the LNSE of NOD.SCID mice (Fig. 3*A*). Similarly, we found that *Deaf1-Var1* expression was not different between the noninflamed cervical lymph nodes (CLNs) of 12-week-old NOD compared with age-matched NOD.B10 mice (Fig. 3*B*), indicating that inflammation in regional nodes may be necessary to induce *Deaf1* splicing at that site.

Next, we induced inflammation in NOD.SCID mice by injecting activated splenocytes from NOD.BDC2.5 mice. NOD.BDC2.5 mice produce highly diabetogenic $CD4^+$ T cells that target the β-cell antigen chromogranin A. Previous studies from our laboratory demonstrated preferential homing of transferred splenocytes to the PLNs and not the CLNs after intraperitoneal injection (25), and our data showed *Ifng* expression was higher in the PLNs of splenocyte-treated mice, confirming that the activated IFN-γ-producing splenocytes homed to the PLNs (Fig. 3*C*).

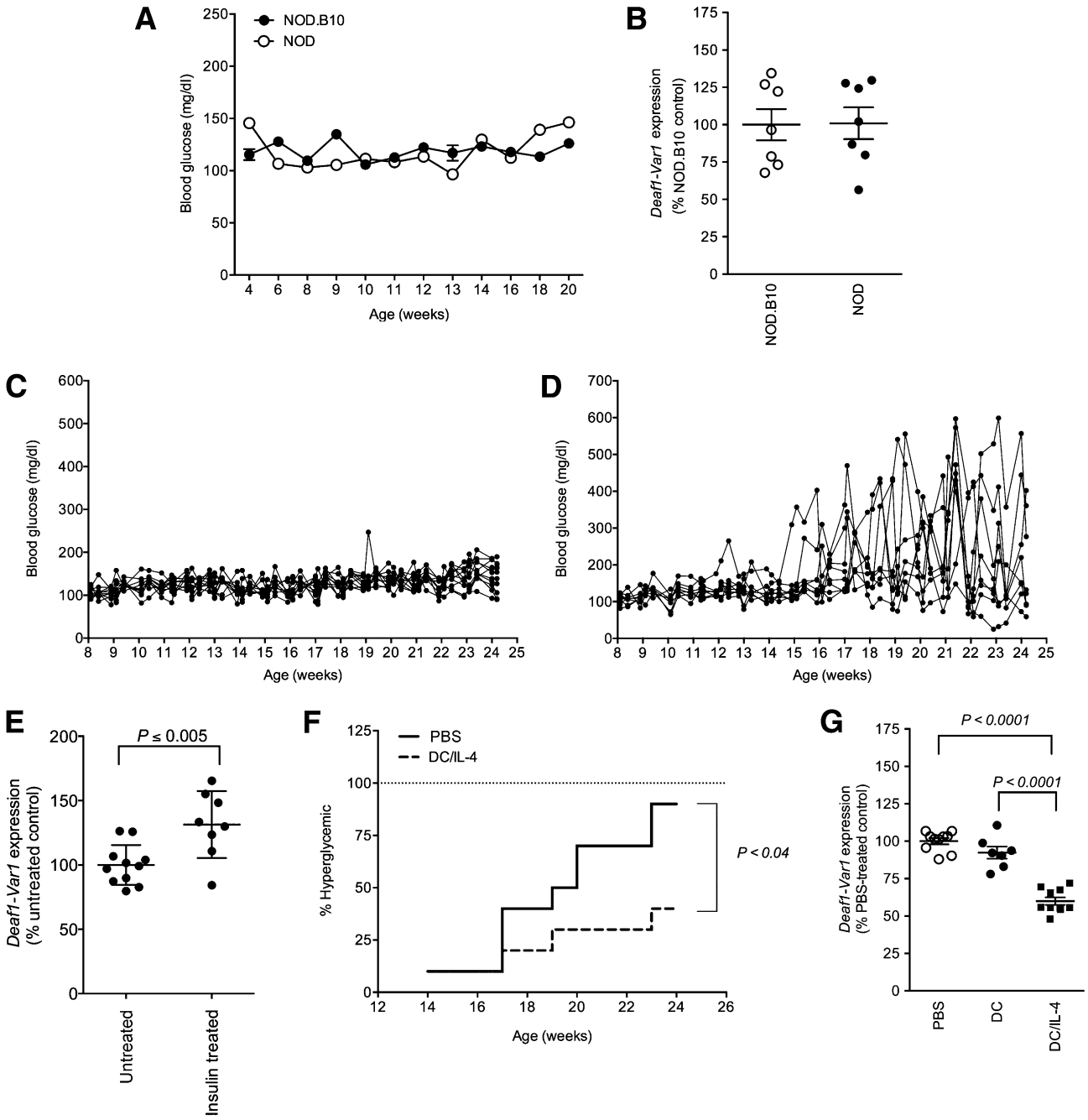

Figure 1—*Deaf1* splicing does not occur in the PLNs of NOD mice that are resistant to or protected from disease, but it does occur in mice that become hyperglycemic. Blood glucose (*A*) and *Deaf1-Var1* expression (*B*) in the PLNs of euglycemic 20-week-old NOD mice compared with NOD.B10 controls ($n = 7$ per group). Data were normalized to *Gapdh* expression. *C–E*: Blood glucose was measured 3 times a week in NOD mice (*C* and *D*). Mice with blood glucose measurements of >375 mg/dL were treated subcutaneously with insulin pellets to maintain survival until 24 weeks of age (see Supplementary Fig. 1 for times of treatment for individual mice). At 24 weeks, *Deaf1-Var1* expression was measured in the PLNs of euglycemic mice (<200 mg/dL; $n = 11$; *C*) and the surviving hyperglycemic insulin-treated mice ($n = 8$; *D*) by QPCR (*E*). *Deaf1-Var1* expression was significantly increased in the insulin-treated hyperglycemic NOD mice. Data were normalized to *18S rRNA* expression. *F*: The incidence of hyperglycemia in NOD mice that were treated at 12 weeks of age with PBS (control) or DCs transfected to express IL-4 (DC/IL-4; $n = 10$ per group). By 24 weeks of age, 90% of control mice (solid line) and 40% of treated mice (dashed line) were hyperglycemic. *G*: QPCR data showing significantly reduced expression of *Deaf1-Var1* in the PLNs of 12-week-old NOD mice 3 days after treatment with DC/IL-4 compared with PBS-treated controls ($n = 10$ per group) and compared with DC-treated controls ($n = 7$). Data were normalized to *Gapdh* expression. The means ± SEM are shown for *A*, *B*, *E*, and *G*. *P* values were determined using the log-rank test (*F*) or the two-tailed unpaired Student *t* test (*B*, *E*, and *G*).

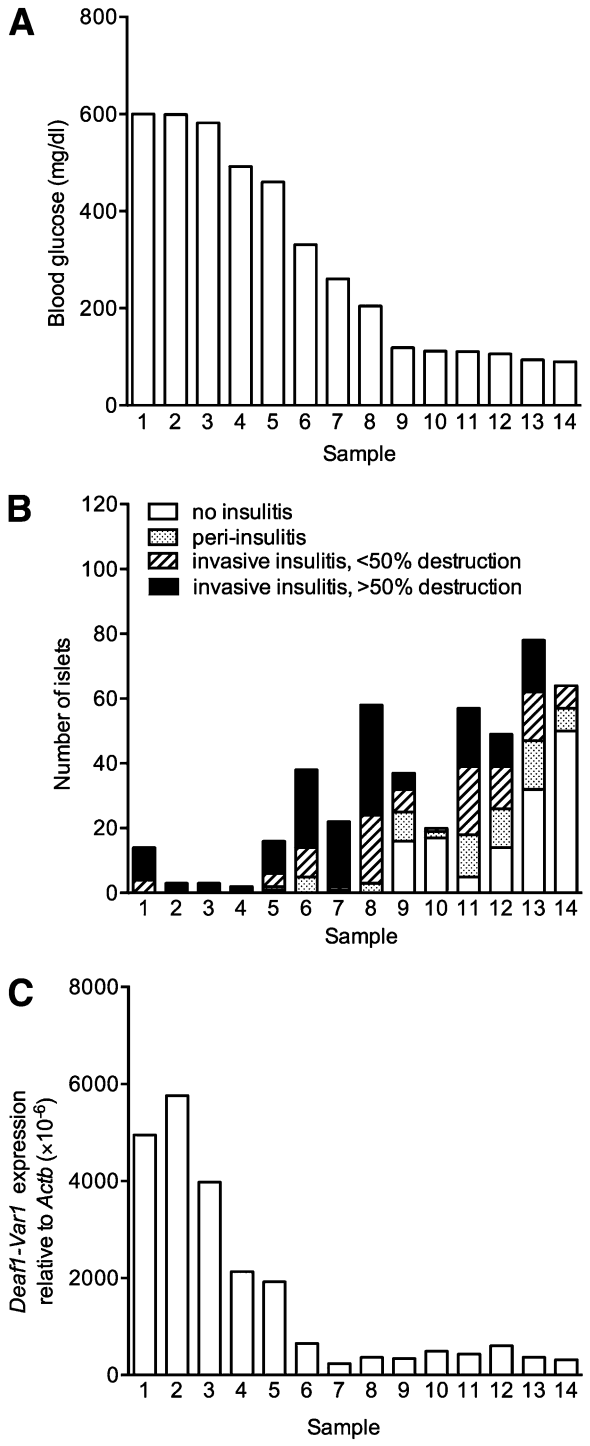

Figure 2—*Deaf1* splicing in NOD PLNs correlates with disease onset and severity. Blood glucose (*A*), insulitis (*B*), and *Deaf1-Var1* expression (*C*) were assessed in the PLNs of 14 individual 16-week-old NOD mice. *Deaf1-Var1* expression was measured by QPCR and shown to correlate strongly with disease severity. Data in *C* were normalized to *Actb* expression.

Deaf1-Var1 expression was also significantly higher in the inflamed PLNs, but not the noninflamed CLNs, of the splenocyte-treated mice compared with PBS-treated control mice (Fig. 3*D* and *E*). Similar results were obtained when NOD.B10 mice were injected with activated splenocytes from NOD.B10 mice (Fig. 3*F–H*). Preferential homing of the activated splenocytes to the PLNs was observed (Fig. 3*F*), and this resulted in *Deaf1* splicing in the PLNs but not in the CLNs (Fig. 3*G* and *H*).

Hyperglycemia Induces the Splicing of *Deaf1* in the PLNs of NOD and NOD.B10 Mice

At 10 weeks of age NOD mice are euglycemic, and *Deaf1-Var1* expression in the PLNs is similar between NOD and NOD.B10 mice (Fig. 4*A*). To assess the impact of hyperglycemia on *Deaf1* splicing, 10-week-old NOD.B10 and NOD mice were treated with the insulin receptor antagonist S961 for 60 h to induce hyperglycemia. Hyperglycemia was established within 24 h and maintained until the mice were killed (Fig. 4*B* and *D*). *Deaf1-Var1* expression was significantly increased in the PLNs of S961-treated NOD.B10 (Fig. 4*C*) and NOD mice (Fig. 4*E*) compared with PBS-treated controls, but it was not significantly changed in the CLNs of these mice (Supplementary Fig. 3*B*). Interestingly, *Deaf1-Var1* was higher in S961-treated NOD mice compared with treated NOD.B10 mice. This may be because of the underlying disease-related inflammation present in the NOD PLNs, as suggested by the slightly higher *Ifng* expression in the PLNs of 10-week-old NOD compared with NOD.B10 mice (Fig. 4*F*). While this amount of inflammation alone is not sufficient to increase the splicing of *Deaf1-Var1* (Fig. 4*A*), it may augment or act synergistically with the effect of hyperglycemia in NOD mice.

Inflammation and Hyperglycemia Mediate *Deaf1* Splicing Through the Activation of Distinct Splicing Factors

Two-color microarray analysis was performed to compare individual PLN samples from 16-week-old NOD mice with severe disease and expressing high levels of *Deaf1-Var1* (Fig. 2*C*, samples 1 and 2) with pooled samples from two normoglycemic NOD mice that expressed extremely low levels of *Deaf1-Var1* (Fig. 2*C*, samples 13 and 14). Of the 41,267 entities on the array, 5,098 were expressed in the PLNs. In samples with high *Deaf1-Var1* expression, only 31 and 15 genes were up- or downregulated, respectively, by fourfold or more compared with samples expressing lower levels of *Deaf1-Var1* (Table 2). GO analysis showed that multiple GO terms, including those related to inflammation and RNA splicing, were significantly linked to the differentially expressed genes (Supplementary Tables 1 and 2).

Interestingly, the genes for two well-studied splicing factors, *Srsf10* and *Ptbp2*, were among those whose expression was most highly upregulated (more than fourfold) and were also linked to RNA splicing (Supplementary Table 2). These two genes are of particular interest because previous work has shown that Srsf10 may bind to a number of glutaraldehyde (GA)-rich motifs that are present in the mouse and human *Deaf1/DEAF1* gene (26), and Ptbp1 (the other member of the Ptbp family) is regulated by

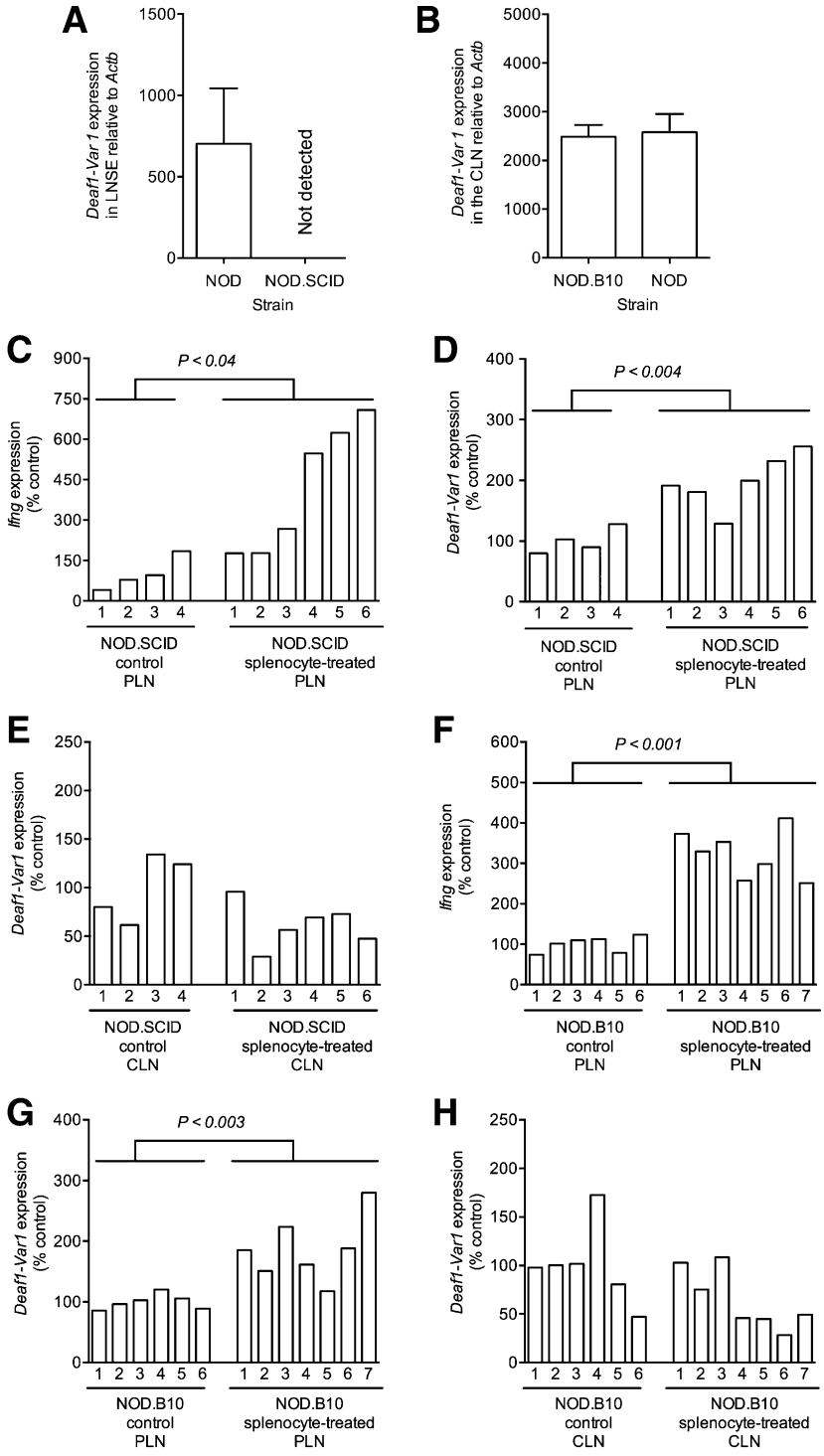

Figure 3—Inflammation induces *Deaf1* splicing in the PLNs. *A*: QPCR data showing expression of *Deaf1-Var1* in inflamed LNSEs extracted from the PLNs of 12-week-old NOD mice but not in the noninflamed tissue of age-matched NOD.SCID mice (means ± SEM). LNSEs were extracted from the pooled PLNs of 5 mice per group. Experiments were performed in triplicate. *B*: QPCR data showing similar levels of *Deaf1-Var1* expression in the noninflamed CLNs of 12-week-old NOD versus NOD.B10 mice. Data in *A* and *B* were normalized to *Actb* expression. *C–E*: QPCR data showing upregulation of *Ifng* (*C*) and *Deaf1-Var1* (*D*) expression in the PLNs of NOD.SCID mice after intraperitoneal injection of activated NOD.BDC2.5 splenocytes. *Deaf1-Var1* expression was not changed in the noninflamed CLNs (*E*). Data were normalized to *18S rRNA* expression. *F–H*: QPCR data showing upregulation of *Ifng* (*F*) and *Deaf1-Var1* (*G*) expression in the PLNs of NOD.B10 mice after intraperitoneal injection of activated NOD.B10 splenocytes. *Deaf1-Var1* expression was not changed in the noninflamed cervical lymph nodes (*H*). Data in *E–G* were normalized to *Actb* expression. In *E–H*, each bar represents an individual mouse, and the *P* values are indicated. Control mice were injected with an equal volume of PBS. Statistical analysis was performed using the Student unpaired *t* test.

the glycemic state (27). These studies suggest that Srsf10 and Ptbp2 may play a role in *Deaf1* splicing in the NOD PLNs. QPCR analysis showed that *Srsf10* and *Ptbp2* expression correlated well with *Deaf1-Var1* expression in the inflamed and hyperglycemic PLNs of 16-week-old NOD mice (Fig. 5*A–C*). Expression of all three genes was significantly higher in hyperglycemic compared with euglycemic 16-week-old NOD mice. In contrast, only *Srsf10* and *Deaf1-Var1* were upregulated in the inflamed PLNs of NOD.SCID mice that were treated with activated splenocytes of NOD.BDC2.5 mice compared with controls (Fig. 5*D–F*). *Ptbp2* expression was unchanged under these inflammatory conditions. Interestingly, expression of *Ptbp2* and *Deaf1-Var1* was significantly increased in the hyperglycemic PLNs of NOD and NOD.B10 mice treated with S961, whereas *Srsf10* expression remained unchanged (Fig. 5*G–L*). These data suggest that inflammation and hyperglycemia may drive *Deaf1* splicing through distinct pathways involving *Srsf10* and *Ptbp2*, respectively. This is consistent with the slightly higher levels of *Srsf10* measured in the hyperglycemic PLNs of NOD mice versus NOD.B10 controls (Fig. 5*H* and *K*).

PTBP2 and SRSF10 Mediate the Splicing of Human *DEAF1* and the Expression of the Putative PTA Gene *CELA1*

To determine whether splicing of human *DEAF1* is also controlled by *PTBP2* and *SRSF10*, plasmids expressing *PTBP2* or *SRSF10* were transfected alone or in combination into HEK293T cells. Transfection increased expression of the corresponding gene and protein within 24 h and was maintained for at least 48 h (Fig. 6*A–C*). Overexpression of *SRSF10* alone resulted in reduced canonical *DEAF1* and increased *DEAF1-VAR1* expression (Fig. 6*D* and *E*). Cotransfection of *PTBP2* with *SRSF10* augmented *DEAF1-VAR1* expression but did not result in additional changes in canonical *DEAF1* expression. This is consistent with our finding that overexpression of *PTBP2* alone increased *DEAF1-VAR1* but did not decrease *DEAF1* expression (Fig. 6*D* and *E*). In all samples studied, *DEAF1* expression was found to be highly abundant compared with *DEAF1-VAR1* expression. Accurate *DEAF1-VAR1* measurements required preamplification of the cDNA. In addition, when measurements were made using TaqMan assays that detected both *DEAF1* and *DEAF1-VAR* (Supplementary Fig. 4), the pattern of change was similar to that seen for *DEAF1* in Fig. 6*D*, indicating that small changes in *DEAF1* expression may account for significant changes in *DEAF1-VAR1* expression. It is also possible (as our preliminary data suggest) that *DEAF1* can be alternatively spliced into other isoforms not detected by the primers used.

We previously showed that *Deaf1* splicing may lead to reduced expression of various islet antigens in the PLNs of NOD mice starting at 12 weeks of age (19), but it is unclear whether *Srsf10* and *Ptbp2* are involved. Here, we questioned whether overexpression of *SRSF10* and/or *PTBP2* could alter PTA expression. Because it is not possible to isolate primary LNSCs without inducing some amount of *Deaf1* splicing, we examined the effect of *SRSF10* and *PTBP2* on the expression of the putative PTA gene chymotrypsin-like elastase family member 1 (*CELA1*) in HEK293T cells. *CELA1* is endogenously expressed in HEK293T cells, whereas other PTA genes, including those encoding insulin, α-1-microglobulin, and fibrinogen, were not detected (data not shown). We previously showed that *Cela1* is concomitantly downregulated with *Deaf1* in the PLNs of 12- and 16-week-old NOD mice relative to NOD.B10 controls (28) and is most abundantly expressed in the double negative ($gp38^-$, $CD31^-$) subset of LNSCs (Supplementary Fig. 5*A* and *B*). Knockout of *Deaf1* almost completely abolishes *Cela1* expression in the double negative subset, indicating that *Cela1* expression is controlled by *Deaf1* (Supplementary Fig. 5*C*). This is consistent with the reduced expression of *Cela1* in the PLNs of NOD.SCID mice that were treated with activated splenocytes and in the PLNs of NOD and NOD.B10 mice that were treated with S961 (Supplementary Fig. 5*D* and *E*). Overexpression of *SRSF10* led to reduced *CELA1* expression in HEK293T cells (Fig. 6*F*). *PTBP2* had no additional effect on *CELA1* when transfected with *SRSF10* and did not alter *CELA1* expression when transfected alone (Fig. 6*F*). Because overexpression of *SRSF10* results in both reduced canonical *DEAF1* expression and increased *DEAF1-VAR1* expression, its overall effect on DEAF1 function is greater than that of *PTBP2* and may explain why increased *SRSF10*, but not *PTBP2*, expression results in reduced *CELA1* expression.

DISCUSSION

T1D can develop from a partial breakdown in peripheral tolerance that is normally controlled by PTA gene expression in LNSCs. We previously showed that Deaf1 controls the expression of various PTA genes in peripheral lymphoid tissues and that diminished Deaf1 function and PTA expression occurs during the onset of destructive insulitis (19). Here, we demonstrate that increased *Deaf1* splicing occurs only in the PLNs of NOD mice that develop hyperglycemia and strongly correlates with the severity of disease. We found that inflammation and hyperglycemia mediate *Deaf1* splicing through the activation of distinct pathways involving the splicing factors Srsf10 and Ptbp2. Our data suggest that during the onset of destructive insulitis at ~12 weeks of age, inflammation in the PLNs upregulates the expression of *Srsf10*, leading to the increased expression of *Deaf1-Var1* and reduced expression of *Deaf1* and PTA genes that is observed in the PLNs (19). As disease progresses and animals become hyperglycemic, *Ptbp2* is upregulated. This induces additional expression of *Deaf1-Var1*. Because deletional tolerance and induction of Tregs may be mediated by PTA expression in LNSCs, diminished Deaf1 function may allow increasing numbers of autoreactive cells to persist during the progression of NOD disease and T1D.

Although the mouse and human isoforms of *Deaf1-Var1* and *DEAF1-VAR1* differ structurally (19), Srsf10/SRSF10

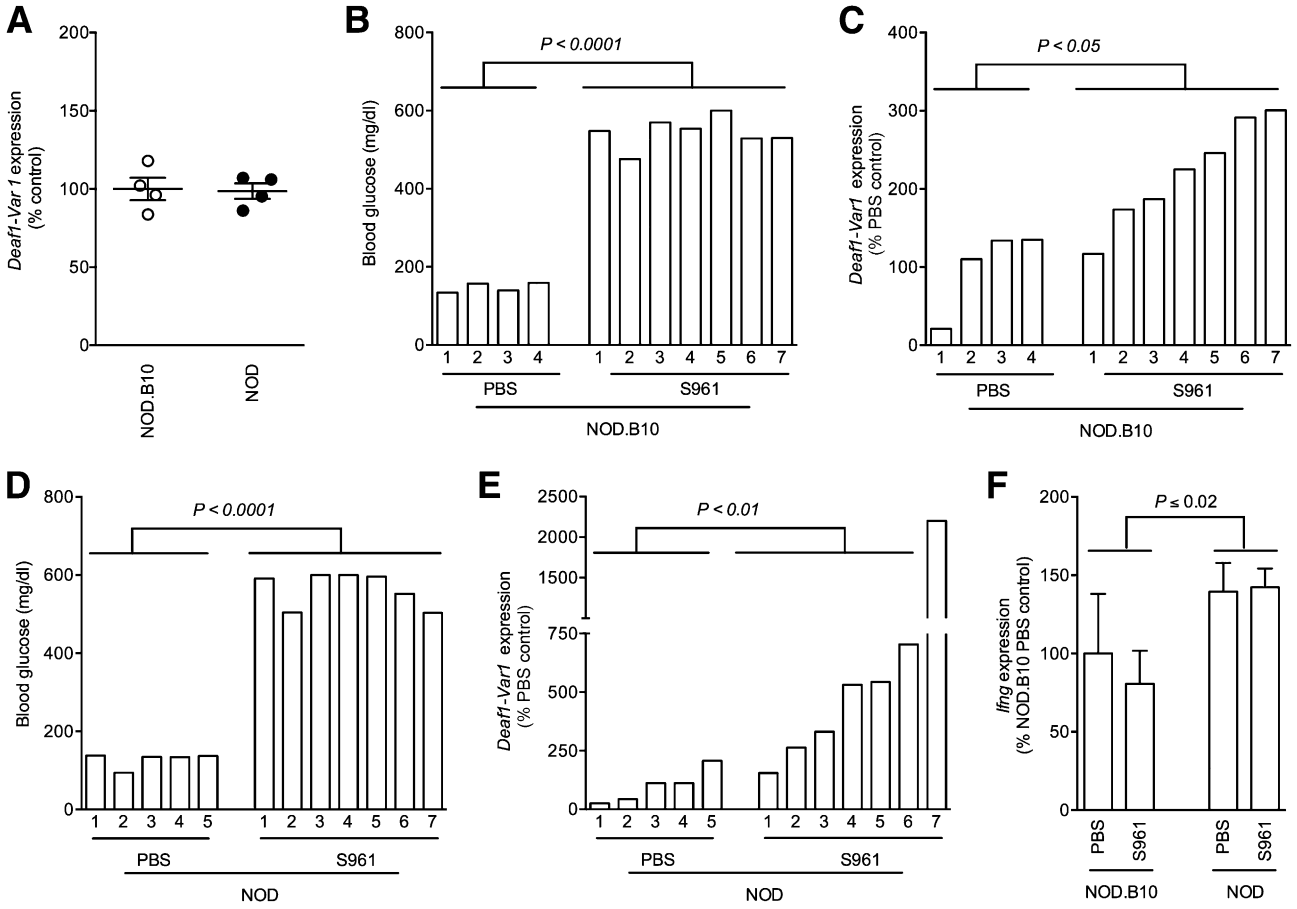

Figure 4—Hyperglycemia induces *Deaf1* splicing in the PLNs. *A*: QPCR data showing the expression of *Deaf1-Var1* in the PLNs of untreated 10-week-old NOD and NOD.B10 mice (means ± SEM; $n = 4$ mice per group). Data were normalized to *Actb* expression. *B–E*: Treatment of 10-week-old NOD.B10 (*B* and *C*) and NOD mice (*D* and *E*) with the insulin receptor antagonist S961 (1.25 nmol/h for 60 h) resulted in hyperglycemia (*B* and *D*) and significantly increased *Deaf1-Var1* expression in the PLNs (*C* and *E*). *F*: *Ifng* expression was significantly higher in the PLNs of NOD mice than NOD.B10 mice. In *B–E*, each bar represents an individual mouse. The same mice were used to generate data shown in *F*. Data in *C*, *E*, and *F* were normalized to *18S rRNA* expression. Control mice were injected with an equal volume of PBS. Statistical analysis was performed using the two-tailed unpaired Student *t* test. *P* values are indicated.

and Ptbp2/PTBP2 may regulate the expression of both. Changes in *SRSF10* elicit a greater effect on *DEAF1* splicing than changes in *PTBP2*; overexpression of *SRSF10* alone upregulated *DEAF1-VAR1* and downregulated both *DEAF1* and the putative PTA gene *CELA1*. We showed that inflammation of the PLNs following injection of activated splenocytes upregulated *Srsf10* in NOD mice. Although the inflammatory mediator involved is unknown, it is likely a soluble factor that is released by activated splenocytes. Studies have shown that inflammation induced by IL-1β and IFN-γ leads to the alternative splicing of ~35% of genes in pancreatic islets. Islets express about 20,000 genes, including various chemokine and cytokine receptors and the majority of all known mammalian splicing factors (20,29,30). Therefore islets are an ideal tissue for studying inflammation-induced gene splicing. Treatment of islets with IL-1β and IFN-γ increases the expression of both *Srsf10* and *Ptbp2* (29). We previously found that the inflamed islets of NOD mice express higher levels of *Srsf10*, but not *Ptbp2*, compared with islets of NOD.B10 mice (GEO series accession no. GSE45897; probe *A_52_P372843* and *A_52_P593110*; Supplementary Fig. 6*A*). Finally, the supernatant of activated NOD.B10 splenocytes upregulated *Deaf1-Var1* expression in isolated NOD.B10 islets, whereas the supernatant of nonactivated splenocytes had no effect (Supplementary Fig. 6*B*). Thus, various inflammatory mediators such as the ones differentially expressed between the supernatant of activated and nonactivated NOD.B10 splenocytes (Supplementary Fig. 6*C*) may modulate *Deaf1* splicing.

DC/IL-4 treatment prevented or delayed disease in 12-week-old NOD mice, as previously described (21), and reversed the splicing of *Deaf1* within 3 days of treatment (Fig. 1*G*). We showed that *Deaf1-Var1* expression was 40% higher in the PLNs of untreated NOD mice. This is comparable to the ~45% higher levels of *Deaf1-Var1* previously

Table 2—Differentially expressed genes in PLNs of 16-week-old NOD mice expressing high levels of *Deaf1-Var1* versus those expressing low levels of *Deaf1-Var1*

Gene symbol	Fold change	Gene description
Genes upregulated by more than fourfold		
Pdpk1	8.21	3-Phosphoinositide-dependent protein kinase-1
1810009J06Rik	7.44	RIKEN cDNA 1810009J06 gene
Ddx25	7.31	DEAD (Asp-Glu-Ala-Asp) box polypeptide 25
Trim55	6.80	Tripartite motif-containing 55
Fbxo31	6.47	F-box protein 31
Hist1h1c	6.38	Histone cluster 1, H1c
Otud3	5.99	OTU domain–containing 3
Ptms	5.93	Parathymosin
Herpud1	5.75	Homocysteine-inducible, endoplasmic reticulum stress–inducible, ubiquitin-like domain member 1
Galntl2	5.39	UDP-N-acetyl-α-D-galactosamine:polypeptide N-acetylgalactosaminyltransferase-like 2 gene
Dcp2	5.08	DCP2 decapping enzyme homolog
H1f0	5.02	H1 histone family, member 0
Glul	4.93	Glutamate-ammonia ligase (glutamine synthetase)
Cwc15	4.88	CWC15 homolog
Tfdp2	4.77	DP-3 protein-regulating cell cycle transcription factor DRTF1/E2F
1110006O24Rik	4.75	RIKEN cDNA 1110006O24 gene
Hist1h1e	4.64	Histone cluster 1, H1e c
Map3k6	4.58	ASK2 mRNA for apoptosis signal-regulating kinase 2
Fbxo2	4.55	F-box protein 2
Srsf10 (Sfrs13a)	**4.51**	**FUS interacting protein (serine-arginine rich) 1**
Reg3b	4.47	Regenerating islet-derived 3 beta
Txnip	4.46	Thioredoxin interacting protein
Gpsm1	4.32	G-protein signaling modulator 1
Fhl1	4.30	Four and a half LIM domains 1
Bbc3	4.27	BCL2 binding component 3
Tfam	4.23	Transcription factor A, mitochondrial gene
Klf15	4.19	Kruppel-like factor 15
Gm11938	4.13	Predicted gene 11938
Ptbp2	**4.07**	**Polypyrimidine tract binding protein 2**
Sesn1	4.05	Sestrin 1
Myo1e	4.03	Myosin IE
Genes downregulated by more than fourfold		
Fabp1	−10.11	Fatty acid binding protein 1
Tgtp1	−5.76	T-cell specific GTPase 1
BC048507	−5.53	cDNA sequence BC048507
Clec2d	−5.15	C-type lectin domain family 2, member d
Traf1	−5.10	TNF receptor-associated factor 1
Lyl1	−4.94	Lymphoblastomic leukemia 1
Neat1	−4.70	Nuclear paraspeckle assembly transcript 1 (nonprotein coding)
Ms4a4b	−4.61	Membrane-spanning 4-domains, subfamily A, member 4B
Amy2a5	−4.44	Amylase 2a5
Ahsg	−4.43	alpha-2-HS-glycoprotein
Sash3	−4.35	SAM and SH3 domain containing 3
Dennd2d	−4.28	DENN/MADD domain containing 2D
Dynll1	−4.23	Dynein light chain LC8-type 1
Lcp1	−4.22	Lymphocyte cytosolic protein 1
Alb	−4.19	Albumin

Data shown are based on the results of two individual arrays. Two-color microarrays were performed separately on PLN RNA samples from mice 1 and 2 (from Fig. 2*C*) with high *Deaf1-Var1* expression compared with a pool of PLN RNA samples from mice 13 and 14 (from Fig. 2*C*) with low *Deaf1-Var1* expression. Boldfaced genes were selected for further analysis.

measured in the PLNs of 12-week-old NOD versus NOD.B10 mice (19). The reestablishment of Deaf1 function is consistent with the normalization of gene expression toward that seen in NOD.B10 PLNs 3 days after treatment (25). Increased Deaf1 function may also explain the larger number of Tregs that was observed in NOD mice treated with DC/IL-4 (21). Which cytokines and splicing pathways mediate the inhibition or reversal of *Deaf1* splicing is unclear. DC/IL-4 treatment skews helper T-cell populations by supporting the function and differentiation of Th2 cells while inhibiting that of Th1 cells (25,31). DC/IL-4 treatment also reduces the ratio of IFN-γ to IL-4

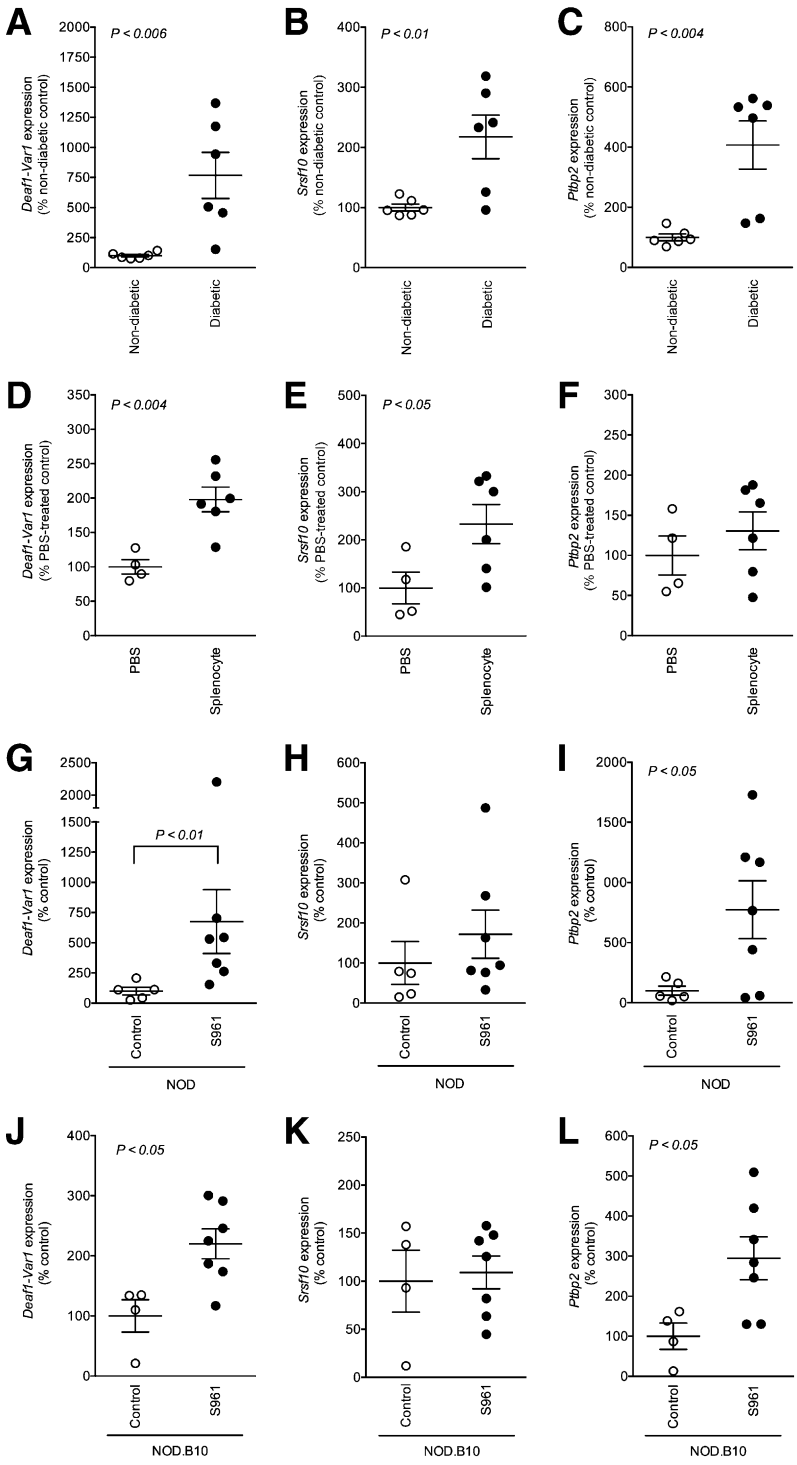

Figure 5—Inflammation and hyperglycemia may mediate *Deaf1* splicing through activation of distinct splicing factors. *A–C*: *Deaf1-Var1* (*A*), *Srsf10* (*B*), and *Ptbp2* expression (*C*) was significantly higher in the PLNs of diabetic (blood glucose >250 mg/dL) 16-week-old NOD mice compared with the PLNs of age-matched nondiabetic (blood glucose <200 mg/dL) NOD mice (n = 6 per group). Data were normalized to *Actb* expression. *D–F*: *Deaf1-Var1* (*D*) and *Srsf10* expression (*E*) was significantly increased in the inflamed PLNs of NOD.SCID mice that were treated with activated splenocytes of NOD.BDC.2.5 mice compared with the noninflamed PLNs of control mice treated with PBS. *Ptbp2* expression (*F*) was not different (n = 4 controls; n = 6 mice treated with splenocytes). *G–L*: *Deaf1-Var1* (*G* and *J*) and *Ptbp2* expression (*I* and *L*) were significantly increased in the hyperglycemic PLNs of S961-treated 10-week-old NOD (*G–I*) and NOD.B10 (*J–L*) mice compared with euglycemic PBS-treated controls. *Srsf10* expression was not significantly changed (*H* and *K*). *G–I*: Data from PBS-treated NOD mice (n = 5) and S961-treated NOD mice (n = 7). *J–L*: Data from PBS-treated NOD.B10 mice (n = 7) and S961-treated NOD.B10 mice (n = 7). Data in *D–I* were normalized to *18S rRNA* expression. The means ± SEM are shown, and statistical analysis was performed using the two-tailed unpaired Student t test. P values are indicated.

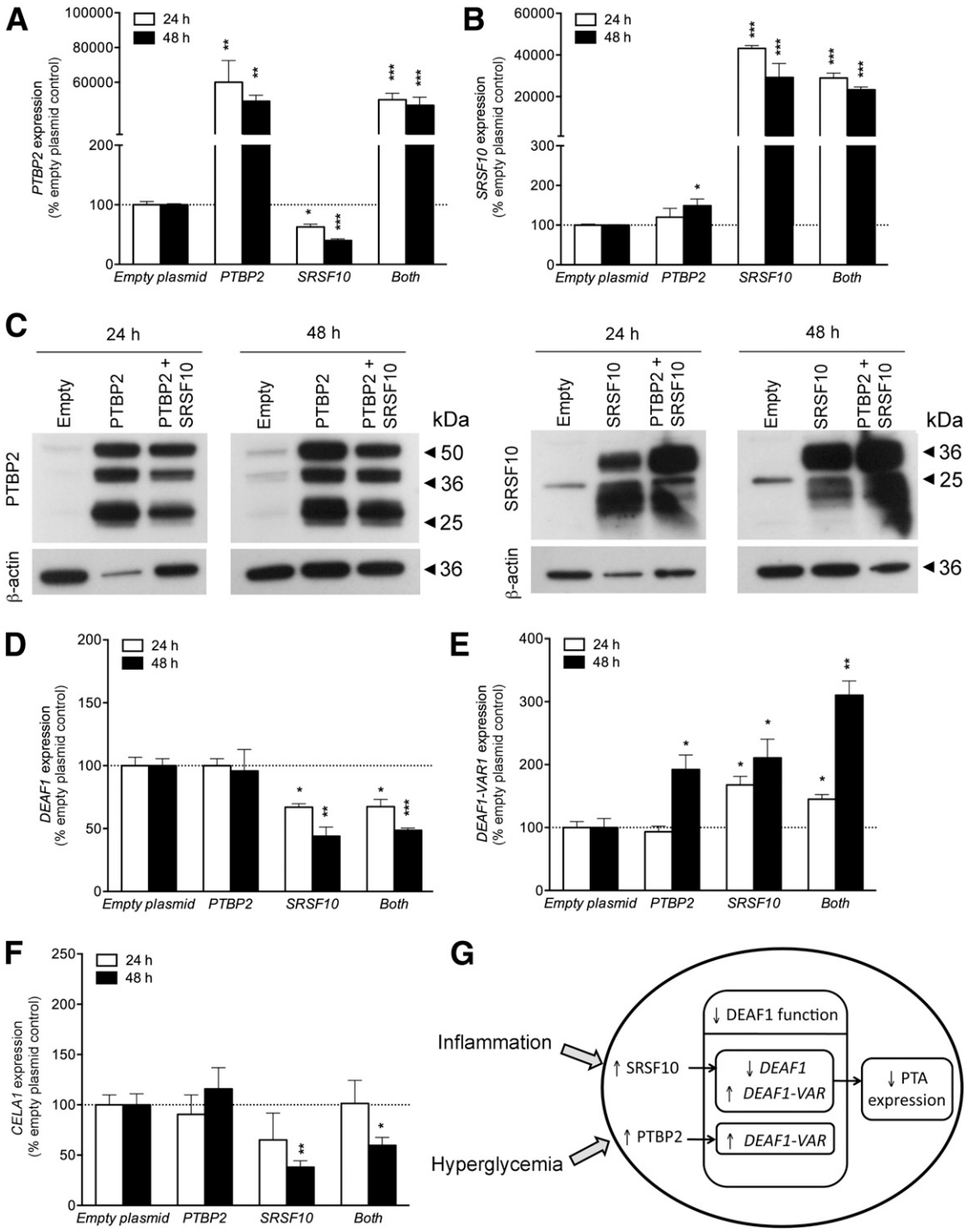

Figure 6—*PTBP2* and *SRSF10* mediate the splicing of human *DEAF1*. *A–F*: QPCR and immunoblotting data showing transfection of HEK293T cells with plasmids expressing *PTBP2* or *SRSF10*, alone (1 μg each) or in combination (0.5 μg each). Transfection resulted in significantly increased mRNA (*A* and *B*) and protein (*C*) expression of the corresponding genes 24 and 48 h after transfection. *C*: The antibodies used detected multiple alternatively spliced isoforms of PTBP2 and SRSF10. The ~57-kDa product detected by the anti-PTBP2 antibody may represent the larger PTBP2 isoforms 1, 2, 3, and/or 4 (predicted size ~57–58 kDa), whereas the 33- and 38-kDa products may represent the smaller PTBP2 isoforms 5 and/or 6 (predicted size ~38 kDa). The 36-kDa product detected by the anti-SRSF10 antibody may represent SRSF10 isoforms 1 and/or 2 (predicted size ~31 kDa), whereas the 20- to 25-kDa products may represent isoforms 3, 4, and/or 5 (predicted size ~20–22 kDa). Overexpression of *SRSF10* alone or in combination with *PTBP2* resulted in significantly reduced expression of canonical human *DEAF1* (*D*), increased expression of *DEAF1-VAR1* (*E*), and reduced expression of the PTA gene *CELA1* (*F*). Overexpression of *PTBP2* resulted only in the increased expression of *DEAF1-VAR1* 48 h after transfection (*E*). *G*: A schematic diagram showing how inflammation and hyperglycemia may contribute to reduced DEAF1 function and reduced PTA expression in LNSCs during the progression of disease. Data shown in *A*, *B*, and *D–F* represent the means ± SEM of at least 3 independent experiments performed in triplicate. *C* shows data that are representative of 4 separate experiments. All QPCR data were normalized to *18S rRNA* expression. Statistical analysis was performed using the two-tailed unpaired Student *t* test. $^{*}P < 0.05$; $^{**}P < 0.01$; $^{***}P < 0.001$.

levels in the PLNs, suggesting that a number of cytokines could play a role. The expression of *Srsf10* and *Ptbp2* was not altered by treatment with DC/IL-4 (data not shown), suggesting that these splicing factors are involved in the upregulation but not the downregulation of *Deaf1* splicing. It is possible that some of the splicing factors listed in Supplementary Table 2 may be involved instead.

Srsf10 is a member of the serine/arginine-rich splicing factor family and functions as a sequence-specific splicing activator. Srsf10 can regulate genes that are involved in apoptosis, cell–stress pathways, or disease development (26). For example, Srsf10 has been shown to regulate the splicing efficiency of the LDL receptor gene, a gene that is differentially expressed in the adipose tissue of streptozotocin-treated mice (32,33). Srsf10 binds to various GA-rich hexamers and mediates specific alternative splicing events based on the position and arrangement of those hexamers (26). Srsf10 can mediate exon inclusion and exclusion by regulating common alternative splicing events such as alternative 5′ or 3′ splice sites, cassette exons, mutually exclusive exons, and retained introns (26). The defining feature of the mouse *Deaf1-Var1* isoform is an intronic insertion between exons 6 and 7 that disrupts the nuclear localization signal. The human *DEAF1-VAR1* isoform also lacks the nuclear localization signal because of a deletion of exon 7 (19). Analysis of the mouse *Deaf1* and human *DEAF1* transcripts shows that they contain at least 18 and 20 of the unique GA-rich hexamers that are recognized by SRSF10, respectively (Supplementary Fig. 7). Thus, it is possible that Srsf10/SRSF10 binds directly to Deaf1/DEAF1 mRNA to mediate its alternative splicing; however, this would need to be confirmed by additional experiments.

The Ptbp family consists of Ptbp1 and Ptbp2. These proteins bind to and stabilize mRNA and can mediate the degradation of mRNA (34). The well-studied Ptbp1 isoform is expressed in a wide range of tissues and is involved in disorders that are characterized by abnormal blood glucose regulation, such as T1D, type 2 diabetes, and obesity (35–38). In healthy individuals, PTBP1 stabilizes preproinsulin mRNA and elevates insulin concentrations in response to hyperglycemia (27,36). Based on our microarray data, *Ptbp1* was not altered in the PLNs of 16-week-old hyperglycemic versus euglycemic NOD mice (96 ± 7%; GEO series GSE57237).

Ptbp2 is expressed in specialized tissues (39,40). This tissue-restricted expression may account for the preferential splicing of *Deaf1* in LNSEs (19), but how Ptbp2 regulates the splicing of Deaf1/DEAF1 is not yet known. Like *Ptbp1*, *Ptbp2* is tightly linked to obesity (37,38) and is stimulated by hyperglycemia (Fig. 5*I* and *L*). Changes in *Ptbp2* expression may be mediated indirectly by hyperglycemia-induced inflammation because hyperglycemia activates various inflammatory pathways, and improper glucose handling is linked with subclinical inflammation (41–45). This would be consistent with the increased *Ptbp2* observed in islets after treatment with IFN-γ and IL-1β (29). Inflammation induced by the injection of activated splenocytes, however, did not alter *Ptbp2* expression in the PLNs of euglycemic mice (Fig. 5*F*). During T1D, increased *Ptbp2* expression would normally occur alongside increased *Srsf10* in the PLNs because inflammation in the PLNs precedes hyperglycemia during the disease process. Increased Ptbp2 would exacerbate the negative effects of Srsf10 on Deaf1 function and PTA expression, as shown in Fig. 6*G*. It is interesting that Ptbp2 and Srsf10 mediate the alternative splicing of both the mouse and human *Deaf1/DEAF1* to form *Deaf1-Var1/DEAF1-VAR1*; the mouse *Deaf1-Var1* isoform results from the inclusion of an intron, whereas the human *DEAF1-VAR1* isoform results from an exclusion of exons (19). Studies have shown that alternative splicing patterns occur in a species-specific manner (46,47); between humans and mice, differences in alternative splicing patterns seem to be driven predominantly by changes in conserved *cis*-regulatory elements, with some contribution from *trans*-acting factors (46).

The data presented here show that *Deaf1* splicing is associated with hyperglycemia and inflammation, but its exact role in disease pathogenesis remains unclear. Further experiments are necessary to examine this. For example, if *Deaf1* splicing is required for the pathogenesis of disease, then blockade of *Deaf1* splicing in the PLNs of NOD mice, perhaps with the use of splice-switching oligomers, as previously described (48), may prevent the onset of hyperglycemia.

Funding. C.G.F. provided the majority of the funding (NIH AI083628). L.Y. has received a Juvenile Diabetes Research Foundation (JDRF) Transitional Award.

Duality of Interest. No potential conflicts of interest relevant to this article were reported.

Author Contributions. L.Y. planned and directed this work, prepared the manuscript and figures, analyzed the data, and performed QPCR, microarray, and histology experiments. R.F. isolated RNA, performed the majority of QPCR and transfection experiments, analyzed the data, and prepared the manuscript. C.T. performed blood glucose measurements and treated mice with insulin and S961. R.J.C. performed the DC/IL-4 experiments, extracted LNSCs, and performed experiments using NOD.B10 splenocytes. T.N.-M. assisted with the DC/IL-4 experiments. C.C.W. and J.M.S. activated splenocytes, collected supernatants, and performed experiments using NOD.BDC.2.5 splenocytes. R.A. performed immunoblotting experiments and isolated RNA from various tissues. M.v.H. coordinated blood glucose measurements and tissue collection from 16-week-old NOD mice. C.G.F. directed this work. All authors reviewed and edited the manuscript. L.Y. and C.G.F. are the guarantors of this work and, as such, had full access to all the data in the study and take responsibility for the integrity of the data and the accuracy of the data analysis.

References

1. Prasad S, Kohm AP, McMahon JS, Luo X, Miller SD. Pathogenesis of NOD diabetes is initiated by reactivity to the insulin B chain 9-23 epitope and involves functional epitope spreading. J Autoimmun 2012;39:347–353

2. Di Lorenzo TP, Peakman M, Roep BO. Translational mini-review series on type 1 diabetes: Systematic analysis of T cell epitopes in autoimmune diabetes. Clin Exp Immunol 2007;148:1–16

3. Gottlieb PA, Delong T, Baker RL, et al. Chromogranin A is a T cell antigen in human type 1 diabetes. J Autoimmun 2014;50:38–41

4. Stadinski BD, Delong T, Reisdorph N, et al. Chromogranin A is an autoantigen in type 1 diabetes. Nat Immunol 2010;11:225–231

5. Wenzlau JM, Juhl K, Yu L, et al. The cation efflux transporter ZnT8 (Slc30A8) is a major autoantigen in human type 1 diabetes. Proc Natl Acad Sci U S A 2007;104:17040–17045
6. Lee JW, Epardaud M, Sun J, et al. Peripheral antigen display by lymph node stroma promotes T cell tolerance to intestinal self. Nat Immunol 2007;8:181–190
7. Nichols LA, Chen Y, Colella TA, Bennett CL, Clausen BE, Engelhard VH. Deletional self-tolerance to a melanocyte/melanoma antigen derived from tyrosinase is mediated by a radio-resistant cell in peripheral and mesenteric lymph nodes. J Immunol 2007;179:993–1003
8. Magnusson FC, Liblau RS, von Boehmer H, et al. Direct presentation of antigen by lymph node stromal cells protects against CD8 T-cell-mediated intestinal autoimmunity. Gastroenterology 2008;134:1028–1037
9. Cohen JN, Guidi CJ, Tewalt EF, et al. Lymph node-resident lymphatic endothelial cells mediate peripheral tolerance via Aire-independent direct antigen presentation. J Exp Med 2010;207:681–688
10. Fletcher AL, Lukacs-Kornek V, Reynoso ED, et al. Lymph node fibroblastic reticular cells directly present peripheral tissue antigen under steady-state and inflammatory conditions. J Exp Med 2010;207:689–697
11. Cohen JN, Tewalt EF, Rouhani SJ, et al. Tolerogenic properties of lymphatic endothelial cells are controlled by the lymph node microenvironment. PLoS ONE 2014;9:e87740
12. Tewalt EF, Cohen JN, Rouhani SJ, et al. Lymphatic endothelial cells induce tolerance via PD-L1 and lack of costimulation leading to high-level PD-1 expression on CD8 T cells. Blood 2012;120:4772–4782
13. Malhotra D, Fletcher AL, Astarita J, et al.; Immunological Genome Project Consortium. Transcriptional profiling of stroma from inflamed and resting lymph nodes defines immunological hallmarks. Nat Immunol 2012;13:499–510
14. Gardner JM, Metzger TC, McMahon EJ, et al. Extrathymic Aire-expressing cells are a distinct bone marrow-derived population that induce functional inactivation of $CD4^+$ T cells. Immunity 2013;39:560–572
15. Bottomley MJ, Collard MW, Huggenvik JI, Liu Z, Gibson TJ, Sattler M. The SAND domain structure defines a novel DNA-binding fold in transcriptional regulation. Nat Struct Biol 2001;8:626–633
16. Jensik PJ, Huggenvik JI, Collard MW. Identification of a nuclear export signal and protein interaction domains in deformed epidermal autoregulatory factor-1 (DEAF-1). J Biol Chem 2004;279:32692–32699
17. Yip L, Creusot RJ, Pager CT, Sarnow P, Fathman CG. Reduced DEAF1 function during type 1 diabetes inhibits translation in lymph node stromal cells by suppressing Eif4g3. J Mol Cell Biol 2013;5:99–110
18. Yip L, Fathman CG. Type 1 diabetes in mice and men: gene expression profiling to investigate disease pathogenesis. Immunol Res 2014;58:340–350
19. Yip L, Su L, Sheng D, et al. Deaf1 isoforms control the expression of genes encoding peripheral tissue antigens in the pancreatic lymph nodes during type 1 diabetes. Nat Immunol 2009;10:1026–1033
20. Yip L, Taylor C, Whiting CC, Fathman CG. Diminished adenosine A1 receptor expression in pancreatic α-cells may contribute to the pathology of type 1 diabetes. Diabetes 2013;62:4208–4219
21. Creusot RJ, Chang P, Healey DG, Tcherepanova IY, Nicolette CA, Fathman CG. A short pulse of IL-4 delivered by DCs electroporated with modified mRNA can both prevent and treat autoimmune diabetes in NOD mice. Mol Ther 2010;18:2112–2120
22. Vikram A, Jena G. S961, an insulin receptor antagonist causes hyperinsulinemia, insulin-resistance and depletion of energy stores in rats. Biochem Biophys Res Commun 2010;398:260–265
23. Shizuru JA, Gregory AK, Chao CT, Fathman CG. Islet allograft survival after a single course of treatment of recipient with antibody to L3T4. Science 1987; 237:278–280
24. Saravia-Fernandez F, Durant S, el Hasnaoui A, Dardenne M, Homo-Delarche F. Environmental and experimental procedures leading to variations in the incidence of diabetes in the nonobese diabetic (NOD) mouse. Autoimmunity 1996;24:113–121
25. Creusot RJ, Yaghoubi SS, Kodama K, et al. Tissue-targeted therapy of autoimmune diabetes using dendritic cells transduced to express IL-4 in NOD mice. Clin Immunol 2008;127:176–187
26. Zhou X, Wu W, Li H, et al. Transcriptome analysis of alternative splicing events regulated by SRSF10 reveals position-dependent splicing modulation. Nucleic Acids Res 2014;42:4019–4030
27. Fred RG, Welsh N. The importance of RNA binding proteins in preproinsulin mRNA stability. Mol Cell Endocrinol 2009;297:28–33
28. Kodama K, Butte AJ, Creusot RJ, et al. Tissue- and age-specific changes in gene expression during disease induction and progression in NOD mice. Clin Immunol 2008;129:195–201
29. Ortis F, Naamane N, Flamez D, et al. Cytokines interleukin-1beta and tumor necrosis factor-alpha regulate different transcriptional and alternative splicing networks in primary beta-cells. Diabetes 2010;59:358–374
30. Eizirik DL, Sammeth M, Bouckenooghe T, et al. The human pancreatic islet transcriptome: expression of candidate genes for type 1 diabetes and the impact of pro-inflammatory cytokines. PLoS Genet 2012;8:e1002552
31. Feili-Hariri M, Falkner DH, Gambotto A, et al. Dendritic cells transduced to express interleukin-4 prevent diabetes in nonobese diabetic mice with advanced insulitis. Hum Gene Ther 2003;14:13–23
32. Swami S, Sztalryd C, Kraemer FB. Effects of streptozotocin-induced diabetes on low density lipoprotein receptor expression in rat adipose tissue. J Lipid Res 1996;37:229–236
33. Ling IF, Estus S. Role of SFRS13A in low-density lipoprotein receptor splicing. Hum Mutat 2010;31:702–709
34. Romanelli MG, Diani E, Lievens PM. New insights into functional roles of the polypyrimidine tract-binding protein. Int J Mol Sci 2013;14:22906–22932
35. Dorajoo R, Blakemore AI, Sim X, et al. Replication of 13 obesity loci among Singaporean Chinese, Malay and Asian-Indian populations. Int J Obes (Lond) 2012;36:159–163
36. Ehehalt F, Knoch K, Erdmann K, et al. Impaired insulin turnover in islets from type 2 diabetic patients. Islets 2010;2:30–36
37. Speliotes EK, Willer CJ, Berndt SI, et al.; MAGIC; Procardis Consortium. Association analyses of 249,796 individuals reveal 18 new loci associated with body mass index. Nat Genet 2010;42:937–948
38. Williams MJ, Almén MS, Fredriksson R, Schiöth HB. What model organisms and interactomics can reveal about the genetics of human obesity. Cell Mol Life Sci 2012;69:3819–3834
39. Markovtsov V, Nikolic JM, Goldman JA, Turck CW, Chou MY, Black DL. Cooperative assembly of an hnRNP complex induced by a tissue-specific homolog of polypyrimidine tract binding protein. Mol Cell Biol 2000;20:7463–7479
40. Xu M, Hecht NB. Polypyrimidine tract-binding protein 2 binds to selective, intronic messenger RNA and microRNA targets in the mouse testis. Biol Reprod 2011;84:435–439
41. Choi HJ, Yun HS, Kang HJ, et al. Human transcriptome analysis of acute responses to glucose ingestion reveals the role of leukocytes in hyperglycemia-induced inflammation. Physiol Genomics 2012;44:1179–1187
42. Colak A, Akinci B, Diniz G, et al. Postload hyperglycemia is associated with increased subclinical inflammation in patients with prediabetes. Scand J Clin Lab Invest 2013;73:422–427
43. Hoffman WH, Burek CL, Waller JL, Fisher LE, Khichi M, Mellick LB. Cytokine response to diabetic ketoacidosis and its treatment. Clin Immunol 2003;108:175–181
44. Stentz FB, Umpierrez GE, Cuervo R, Kitabchi AE. Proinflammatory cytokines, markers of cardiovascular risks, oxidative stress, and lipid peroxidation in patients with hyperglycemic crises. Diabetes 2004;53:2079–2086
45. de Rekeneire N, Peila R, Ding J, et al. Diabetes, hyperglycemia, and inflammation in older individuals: the health, aging and body composition study. Diabetes Care 2006;29:1902–1908
46. Barbosa-Morais NL, Irimia M, Pan Q, et al. The evolutionary landscape of alternative splicing in vertebrate species. Science 2012;338:1587–1593
47. Merkin J, Russell C, Chen P, Burge CB. Evolutionary dynamics of gene and isoform regulation in Mammalian tissues. Science 2012;338:1593–1599
48. Fuhlbrigge R, Yip L. Self-antigen expression in the peripheral immune system: roles in self-tolerance and type 1 diabetes pathogenesis. Curr Diab Rep 2014;14:525